Modelling Performance and Emissions Characteristics of CI Engines Running on Tropical Almond Seed-Based Biodiesel

N. B. Jagunmolu[1, 2], S. K. Fasogbon[1]

[1]*Department of Mechanical Engineering, University of Ibadan, Ibadan, Nigeria*
[2]*Centre for Petroleum, Energy Economics and Law, University of Ibadan, Nigeria*

Abstract*: There are growing numbers of countries in the world whose sources of their energy still largely depend on fossil fuels. Unfortunately, these are non-renewable fuels and their integrity is being questioned because of their high carbon emissions and the link they have with global warming. Researchers therefore find it necessary to find different energy sources that have no or low carbon emissions; and one of such alternative sources found to mitigate global warming syndrome is the use of biodiesel to either compliment or replace fossil fuels in Compression ignition engines. Also; emissions characteristics of CI engines have been found to be affected by fuel injection parameters, and this is specific for each type of fuel run on the engine. This work therefore employed the use of GT-Power computer simulation package to study the impact of varying injection timing on emission characteristics of a compression ignition engine fueled with Tropical Almond Seed based Biodiesel and its blends. At compression ratio of 17.5 and varying engine speed of 1000 rpm to 5000rpm; the study examined the impact over a Kirloskar four-stroke, single-cylinder, water-cooled, direct-ignition, compression-ignition engine fueled with tropical almond seed oil-based biodiesel and its blends B0 to B100 at 5% incremental step and four separate injection timings (21◦, 23◦, 25◦, 27◦CA BTDC). The results showed a considerable increase of CO2; and decrease in HC and CO and for tropical almond oil-based biodiesel and its blends at advanced injection timing of 27 bTDC. NOx emissions also slightly increased with the increase in biodiesel content and injection timing at higher speeds. For all blends tested, B35 provides the best result in terms of lowest HC for all investigated injection timings. The study therefore concludes that for better emission profile, Tropical almond seed oil-based biodiesel blend; B35 at 27◦CA BTDC CI engine injection timing provides a good mix.

***Keywords*— injection timing; tropical almond seed; performance; emission; GT-Power; compression ignition engine**

Nomenclature

PV – Photovoltaic	**WCOME – Waste cooking oil methyl ester**
GHG – Greenhouse gas	**GT – Gamma technologies**
MOME – Mahua oil methyl ester	**IMEP – Indicated mean effective pressure**
DI – Direct injection	**BT – Brake torque**
BTE – Brake thermal efficiency	**ISFC – Indicated specific fuel consumption**
BSFC – Brake specific fuel consumption	**bTDC – Before top dead centre**
BMEP – Brake mean effective pressure	**HC – Hydrocarbon**
PM – Particulate matter	**BP – Brake power**
P_{max} – Maximum pressure	**CO – Carbon monoxide**
HRR_{max} – Maximum heat release rate	**NO_X – Oxides of nitrogen**
IT – Injection timing	**IP – Injection pressure**
CA – Crank angle	

I. INTRODUCTION

The demand for energy is increasing day by day due to security, industrial and human development. There are a growing number of countries in the world facing what is called an energy deficit. The gap is widening due to the deliberate removal of fossil fuels. However, these are non-renewable and are being questioned because of their carbon emissions and the link they have to global warming. According to Renewables-2018 IEA (International Energy Agency), bioenergy will remain the predominant source of renewable energy, although its share of total energy declines from 50%, in 2017, to 46% as the expansion of both solar PV and wind accelerates in the electricity sector. Also, the share of renewables in meeting global energy demand is expected to grow by one-fifth in the next five years to reach 12.4% in 2030. It is, therefore, necessary to find different energy sources, which is why they use renewable energy sources in the energy world is a new trend. One of the alternative sources of renewable energy is the use of biodiesel which is environmentally friendly and enables a reduction of greenhouse gas emissions. Apart from reducing GHG emissions, a need to improve the performance and emission characteristics of a compression ignition engine fueled with biodiesel comes to play.

Different studies have been considered for a compression ignition engine fueled with different biodiesel and its blend with diesel. In the work of (Orhevba et al., 2016), tropical almond seed oil was converted to biodiesel through the transesterification process using 25ml of methanol against

100ml of oil in the ratio of 4:1 and 0.7g of KOH as the catalyst. The biodiesel samples produced were then tested to determine the quality of the biodiesel as a diesel fuel substitute (ASTM). They deduced that the majority of the properties fell within the ASTM standard limits for biodiesel. They further reported that since the properties of biodiesel from tropical almond seed oil met the standard for biodiesel, tropical almond biodiesel can be used as an alternative fuel in diesel engines. [2] analyzed the performance and emission characteristics of a castor biodiesel/diesel blends (2%, 5%, and 10%) in a 4.4 kW single-cylinder, air-cooled four-stroke compression ignition engine at various loads. It was observed that performance characteristics like thermal brake efficiency (BTE), brake specific fuel consumptions (BSFC) with 10% Castor methyl ester was closed to diesel fuel while CO, HC and smoke were lower compared to diesel fuel. Although NOx emission was observed to be higher for Castor biodiesel blends. Furthermore, (Babulal et al., 2015) investigated the performance and emission analysis of Compression Ignition (CI) engine fueled with biodiesel (B40 and B100) and petroleum diesel fuel. It was observed that BSFC for brake power (0.5 KW) with petroleum diesel, B40 and B100 were 0.46 kg / kWh, 0.5 kg / kWh and 0.62 kg / kWh respectively while BTE at full load (3.75 kW) with petroleum diesel, B40 was close to 33 %, but BTE with B100 was about 28 %. Also, NO_X with B40 was increased by 2 % when compared to petroleum diesel, whereas with B100 it was about 10 %. Furthermore, CO decreased by 20% with B40 and about 50 % with B100. It was concluded that biodiesel mixture of B40 could be the best substitute for petroleum diesel.

The literature revealed that fuel injection parameters influence engine performance and emission characteristics in a compression ignition engine, and this is specific for each fuel run on the engine. In the work of [4], an experimental investigation was carried out on a single-cylinder four-stroke diesel engine fueled with Mahua (B50) biodiesel-nanoparticle blends at different fuel injection pressures (200, 220 and 240 bar) and fuel injection (19°, 23° and 27° bTDC) timings to determine performance and emission characteristics. It was found that injecting fuel at 240 bar, and 19° bTDC gave better engine performance and emissions with the Brake thermal efficiency and BSFC improved by 21.8% and 12% respectively when compared to diesel while CO (%), HC (ppm) and Smoke opacity (%) were decreased by 52.94%, 62.22%, 28.22% respectively but increased by 6.39% when compared to diesel for NO_X (ppm). In another separate study, (Hwang et al., 2014) led the engine tests of waste cooking oil biodiesel on a single-cylinder, direct injection diesel engine. In their study, the effects of different injection pressures (80 and 160 MPa) and injection timing (25-0 ° CA BTDC) on the combustion and emission characteristics of the engine at two different engine loads were investigated. Their results showed that P_{max} and HRR_{max} were slightly lower for the biodiesel injection timings, while ID was slightly longer. Also, improvements in smoke, CO, HC emissions were found at higher fuel injection pressures, while NOx emissions were increased. [6] examined the effect of injection pressure and injection timing on the WCO biodiesel single-cylinder DI diesel engine. The results showed that the combined effect of higher injection pressure and advanced injection timing significantly improved the brake thermal efficiency. Decreases in nitric oxide (NO) and smoke emissions were also observed.

[7] critically studied the influence of injection timing on engine performance and exhaust emissions of B20+25ppm (20% methyl ester Mimusops Elangi-80% diesel + 25 ppm of TiO_2 nanoparticles) as an alternative fuel. The performance and exhaust emissions of CI engine at the different injection timings for B20+25ppm at retard injection timings (RIT) of CA19 deg bTDC, CA21 deg bTDC and advanced injection timings of CA25 deg bTDC, CA27 deg bTDC with reference to standard injection timing of CA23 deg bTDC was investigated. They observed that at retarded injection timing B20 +25 ppm TiO2 there was an increase in HC and CO emissions, but a decrease in NO_X emissions when the injection time was delayed. Advancing injection timing for the nanoparticle additive B20 +25 ppm TiO2 reflected in an increase in the thermal efficiency of the brakes, a reduction in the specific fuel consumption of the brakes and a reduction in HC emissions, CO and smoke, with a marginal increase in NO_X emissions. [8] assessed engine performance and emission conditions with advanced and delayed fuel injection timing on a CI diesel engine by modifying the injection timing (i.e. 4 degrees before and after the actual injection timing of 23 degrees bTDC) under different load conditions. The biodiesel mixture was prepared with the mixture ratio of 25% biodiesel and 75% diesel, then added 100 ppm of alumina nanoparticles to operate the diesel engine. They observed that at advanced injection timing of 27 deg bTDC, the performance of an engine was improved, but exhaust gases such as hydrocarbons, carbon monoxide and smoke emissions were reduced and nitrogen oxide emissions increased slightly compared to regular diesel. [9] evaluated the use of rubber seed oil with diesel at a proportion of 20% by volume (RSO20) in a four-stroke single-cylinder compression ignition engine cooled by air with constant injection and constant speed (1500 rpm) at different injection times (24 °, 27 °, 30 °, 33 ° bTDC (before top dead centre)). They reported that at full load, the thermal efficiency of the RSO20 brake at 30 ° bTDC is high compared to other injection settings and fuel consumption is increased during advanced injection timing. Also, a significant reduction in unburnt hydrocarbon and carbon monoxide emissions, and an increase in emissions of nitrogen oxides (NOx) was observed as the injection timing advances. [10] used a single-cylinder CI engine to test the two biodiesel samples of rice bran oil methyl esters (ROME) and algae oil methyl esters (AME) for their combustion characteristics at constant speed (1500 rpm) with three

different injection settings (20 ° before top dead centre [BTDC], 23 ° BTDC and 26 ° BTDC). They observed an increase in the cylinder pressure and the rate of heat generation at advanced injection timing during the previous combustion stages. Also, at retarded injection timing, the cylinder pressure and the rate of heat generation decreased. They concluded that combustion characteristics of ROME showed better results compared to AME.

[11] studied TSME 20 (20% methyl ester of tamarind seeds and 80% diesel) as an alternative fuel and its performance and emission characteristics in a diesel engine at different injection timing (19 °, 23 ° and 27 ° bTDC) and different loads. At full load, a considerable improvement in the thermal efficiency of the brakes of 3.18% was observed with a significant reduction in carbon monoxide, hydrocarbons, nitrogen oxides and smoke 17.3%, 57.3%, 31.34% and 8.1%, respectively, at retarded injection timing compared to the standard injection timing. [12] observed the performance and the emission characteristics of a four-stroke direct injection single cylinder diesel engine using methyl esters of linseed oil and mixtures thereof B10, B20 with a power of 5.2 kW at 1500 rpm at various injection timing, 20, 23, 26 degrees BTDC. It was reported that compared to diesel, the blends gave an increase in BTHE and a reduction in SFC. Also, the two biodiesel blends gave less NOx but slightly higher CO and HC emissions were found. It was concluded that performance and emissions increased as the injection timing increased. In the work of (Fasogbon et al., 2019), performance tests were performed on a single-cylinder four-stroke water-cooled compression ignition engine on different percentages of a mixture of tropical almond ester and diesel at different injection times. The engine's forward-transmitted Levenberg-Marquardt algorithm was used to estimate engine performance characteristics using a modelled artificial neural network (ANN). The mix variables, load percentage, and injection timing were used as input variables for network development, while engine performance parameters (brake thermal efficiency, exhaust temperature, and brake specific fuel consumption) were used as output variables. The experimental results obtained were used to train the network structure. An excellent correlation between the predicted values of ANN and the desired values was obtained for different engine performance ratings. The average relative error values obtained were less than 10%. It was concluded that ANN is an accurate predictor of engine performance.

Additionally, (Rahim et al., 2010) compared the performance of a Mitsubishi 4D68, a four-cylinder, 50 kW direct-injection engine powered by biodiesel and diesel fuels using the GT power software. It was reported that biodiesel generally has lower torque and power output than diesel. (Fasogbon & Odia, 2019) also studied the combustion characteristics of turbocharged low heat rejection direct injection compression ignition engine fueled with biodiesel from Terminalia Catappa L. and its blends using MATLAB software. It was reported that crank angle and blends of biodiesel increase enhances combustion characteristics. From the review of literature, it can be seen that while lot of work has been carried out to improve the performance and emission of biodiesel fuelled compression ignition engine. Literature is sparse on tropical almond-based biodiesel, to this end, this paper presents a simulation study to investigate the impact of injection timing on the performance and emission characteristics of a compression ignition engine fueled with Tropical Almond Seed Biodiesel and its blends. Results are analyzed with respect to diesel.

II. SIMULATION MODEL

GT-POWER a major manufacturers standard engine simulation software is used in the industry to predict performance, emission and acoustic characteristics of an engine. Predictions are extended to include control system modelling, in-cylinder and pipe/manifold structure temperature and cylinder pressure analysis. It is based on one-dimensional modelling from GT-SUITE. Fig. 1 shows the developed engine model of a single-cylinder, direct injection compression ignition engine.

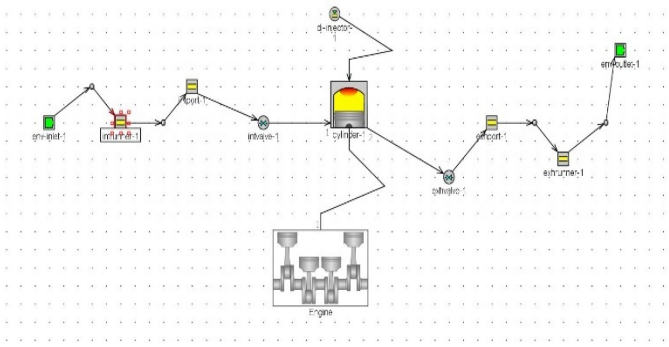

Fig. 1 Engine model

In the present work, the performance and emissions characteristics of a Kirloskar make diesel engine was studied with GT-Power software at different blend ratio and various injection timings. The engine specifications can be found in Table I. The experimental data given in Table II for biodiesel used in this work were gotten from the work of (Fasogbon & Odia, 2019). The critical temperature and pressure of linoleic acid given in Table III for biodiesel used in this work were gotten from the work of (Sahasrabudhe et al., 2017), in which the critical properties of No. 2 diesel were obtained from the GT-Power fuel library. The physiochemical properties of the blended fuel were calculated by interpolating between the physiochemical properties of Diesel (B0) and Biodiesel (B100), given in Table IV based on the observation by most researchers that fuel properties of blends very linearly. The biodiesel properties calculated include critical properties, density, entropy, enthalpy, the heat of vaporization, dynamic viscosity, thermal conductivity, lower heating value, and molecular chemical structure.

Table I: Engine Specification

Engine parameters	Specification
Make	Kirloskar
Model/type	TVI/Four Stroke
Number of Cylinders	Single
Bore	87.5mm
Stroke	110mm
Rated Output	5.2 kW (7 hp)
Rated speed	1500RPM
Cubic Capacity (cc)	661
Type of cooling	Water cooling
Compression ratio range	17.5:1
Injection timing	23 bTDC
Torque at Full Load	0.033 kN-m
Injection mass	60mg
Number of injector nozzle holes	3
Connecting rod	230mm

Table II: Physiochemical Properties Of Tropical Almond

Properties	Diesel	Biodiesel
Density @ 20 ^{0}C (kg/m^3)	830	888
Cetane number	48	51.70
Viscosity @ 40 ^{0}C (mm^2/s)	2.8	4.31
Flash point @ 40 ^{0}C	55	145.3
Lower Heating Value (MJ/kg)	43.25	36.97

Table III: Fuel Properties Used In Gt-Power

Blends			C	H	O	Tc(K)	Pc(bar)	Entropy (J/Kg.K)	HOV (J/Kg)	Vap_entropy (J/Kg.k)	Enthalpy Coefficient (a1)
B0	0.00	1	13.5	23.6	0	569.4	24.6	2913.25	250000	3445.47	2050
B5	0.05	0.95	13.725	24.02	0.1	581.921	24.0355	2884.59	253500	3411.571	2029.85
B10	0.10	0.9	13.95	24.44	0.2	594.442	23.471	2855.93	257000	3377.672	2009.7
B15	0.15	0.85	14.175	24.86	0.3	606.963	22.9065	2827.26	260500	3343.773	1989.55
B20	0.20	0.8	14.4	25.28	0.4	619.484	22.342	2798.6	264000	3309.874	1969.4
B25	0.25	0.75	14.625	25.7	0.5	632.005	21.7775	2769.94	267500	3275.975	1949.25
B30	0.30	0.7	14.85	26.12	0.6	644.526	21.213	2741.28	271000	3242.076	1929.1
B35	0.35	0.65	15.075	26.54	0.7	657.047	20.6485	2712.61	274500	3208.177	1908.95
B40	0.40	0.6	15.3	26.96	0.8	669.568	20.084	2683.95	278000	3174.278	1888.8
B45	0.45	0.55	15.525	27.38	0.9	682.089	19.5195	2655.29	281500	3140.379	1868.65
B50	0.50	0.5	15.75	27.8	1	694.61	18.955	2626.63	285000	3106.48	1848.5
B55	0.55	0.45	15.975	28.22	1.1	707.131	18.3905	2597.96	288500	3072.581	1828.35
B60	0.60	0.4	16.2	28.64	1.2	719.652	17.826	2569.3	292000	3038.682	1808.2
B65	0.65	0.35	16.425	29.06	1.3	732.173	17.2615	2540.64	295500	3004.783	1788.05
B70	0.70	0.3	16.65	29.48	1.4	744.694	16.697	2511.98	299000	2970.884	1767.9
B75	0.75	0.25	16.875	29.9	1.5	757.215	16.1325	2483.31	302500	2936.985	1747.75
B80	0.80	0.2	17.1	30.32	1.6	769.736	15.568	2454.65	306000	2903.086	1727.6
B85	0.85	0.15	17.325	30.74	1.7	782.257	15.0035	2425.99	309500	2869.187	1707.45
B90	0.90	0.1	17.55	31.16	1.8	794.778	14.439	2397.33	313000	2835.288	1687.3
B95	0.95	0.05	17.775	31.58	1.9	807.299	13.8745	2368.66	316500	2801.389	1667.15
B100	1.00	0	18	32	2	819.82	13.31	2340	320000	2767.49	1647

Table IV: Heating Value Properties

	Blends(X)	LHV (*10^6) MJ/kg	Density@20*C(kg/m^3)
B0	0	43.25	830
B5	0.05	42.936	833.0048
B10	0.1	42.622	835.8191
B15	0.15	42.308	838.6334
B20	0.2	41.994	843
B25	0.25	41.68	844.2619
B30	0.3	41.366	847.0762
B35	0.35	41.052	849.8905
B40	0.4	40.738	852
B45	0.45	40.424	855.5191
B50	0.5	40.11	858.3334
B55	0.55	39.796	861.1476
B60	0.6	39.482	863
B65	0.65	39.168	866.7762
B70	0.7	38.854	869.5905
B75	0.75	38.54	872.4048
B80	0.8	38.226	874
B85	0.85	37.912	878.0334
B90	0.9	37.598	880.8476
B95	0.95	37.284	883.6619
B100	1	36.97	888

The dynamic viscosity array given in Table V – VI for almond biodiesel used in this work were gotten from the work of [17], in which the properties of No. 2 diesel were obtained from the GT-Power fuel library.

Table V: Dynamic Array

Dynamic Array											
T(K)	B0	B5	B10	B15	B20	B25	B30	B35	B40	B45	B50
273.15	0.00219	0.003930975	0.00567195	0.007412925	0.0091539	0.010894875	0.01263585	0.014376825	0.0161178	0.017858775	0.01959975
290.15	0.00171	0.003279475	0.00484895	0.006418425	0.0079879	0.009557375	0.01112685	0.012696325	0.0142658	0.015835275	0.01740475
310.15	0.00133	0.002688475	0.00404695	0.005405425	0.0067639	0.008122375	0.00948085	0.010839325	0.0121978	0.013556275	0.01491475
330.15	0.0011	0.002239975	0.00337995	0.004519925	0.0056599	0.006799875	0.00793985	0.009079825	0.0102198	0.011359775	0.01249975
350.15	0.00096	0.001876975	0.00279395	0.003710925	0.0046279	0.005544875	0.00646185	0.007378825	0.0082958	0.009212775	0.01012975
373.15	0.00088	0.001536475	0.00219295	0.002849425	0.0035059	0.004162375	0.00481885	0.005475325	0.0061318	0.006788275	0.00744475
400.15	0.00087	0.001216475	0.00156295	0.001909425	0.0022559	0.002602375	0.00294885	0.003295325	0.0036418	0.003988275	0.00433475
450.15	0.00112	0.001249	0.001378	0.001507	0.001636	0.001765	0.001894	0.002023	0.002152	0.002281	0.00241

Table VI: Dynamic Array

Dynamic Array										
T(K)	B55	B60	B65	B70	B75	B80	B85	B90	B95	B100
273.15	0.021340725	0.0230817	0.024822675	0.02656365	0.028304625	0.0300456	0.031786575	0.03352755	0.035268525	0.0370095
290.15	0.018974225	0.0205437	0.022113175	0.02368265	0.025252125	0.0268216	0.028391075	0.02996055	0.031530025	0.0330995
310.15	0.016273225	0.0176317	0.018990175	0.02034865	0.021707125	0.0230656	0.024424075	0.02578255	0.027141025	0.0284995
330.15	0.013639725	0.0147797	0.015919675	0.01705965	0.018199625	0.0193396	0.020479575	0.02161955	0.022759525	0.0238995
350.15	0.011046725	0.0119637	0.012880675	0.01379765	0.014714625	0.0156316	0.016548575	0.01746555	0.018382525	0.0192995
373.15	0.008101225	0.0087577	0.009414175	0.01007065	0.010727125	0.0113836	0.012040075	0.01269655	0.013353025	0.0140095
400.15	0.004681225	0.0050277	0.005374175	0.00572065	0.006067125	0.0064136	0.006760075	0.00710655	0.007453025	0.0077995
450.15	0.002539	0.002668	0.002797	0.002926	0.003055	0.003184	0.003313	0.003442	0.003571	0.00370

Table VII: Thermal Array

Thermal array											
T(K)	B0	B5	B10	B15	B20	B25	B30	B35	B40	B45	B50
273.15	0.116645	0.118403109	0.1201612	0.121919327	0.12367744	0.125435545	0.1271937	0.128952	0.130709872	0.132467981	0.13422609
290.15	0.113925	0.115871931	0.1178189	0.119765792	0.12171272	0.123659653	0.1256066	0.127554	0.129500445	0.131447375	0.133394306
310.15	0.110725	0.112894074	0.1150631	0.117232221	0.11940129	0.121570368	0.1237394	0.125909	0.128077589	0.130246662	0.132415736
330.15	0.107525	0.109916217	0.1123074	0.11469865	0.11708987	0.119481083	0.1218723	0.124264	0.126654733	0.129045949	0.131437166
350.15	0.104325	0.10693836	0.1095517	0.112165079	0.11477844	0.117391798	0.1200052	0.122619	0.125231877	0.127845236	0.130458596
373.15	0.100645	0.10351275	0.1063805	0.10924825	0.112116	0.11498375	0.1178515	0.120719	0.123587	0.12645475	0.1293225
400.15	0.096325	0.099493717	0.1026624	0.105831151	0.10899987	0.112168585	0.1153373	0.118506	0.121674737	0.124843454	0.128012171
450.15	0.088325	0.092049075	0.0957731	0.099497224	0.1032213	0.106945373	0.1106694	0.114394	0.118117597	0.121841671	0.125565746

Table VIII: Thermal Array

Thermal array										
T(K)	B55	B60	B65	B70	B75	B80	B85	B90	B95	B100
273.15	0.1359842	0.137742308	0.1395004	0.141258526	0.14301664	0.144774744	0.1465329	0.148291	0.150049071	0.15180718
290.15	0.13534124	0.137288167	0.1392351	0.141182028	0.14312896	0.145075889	0.1470228	0.14897	0.150916681	0.152863611
310.15	0.13458481	0.136753883	0.138923	0.14109203	0.1432611	0.145430177	0.1475993	0.149768	0.151937398	0.154106471
330.15	0.13382838	0.136219599	0.1386108	0.141002032	0.14339325	0.145784465	0.1481757	0.150567	0.152958115	0.155349331
350.15	0.13307196	0.135685315	0.1382987	0.140912034	0.14352539	0.146138753	0.1487521	0.151365	0.153978832	0.156592191
373.15	0.13219025	0.135058	0.1379258	0.1407935	0.14366125	0.146529	0.1493968	0.152265	0.15513225	0.158
400.15	0.13118089	0.134349605	0.1375183	0.140687039	0.14385576	0.147024473	0.1501932	0.153362	0.156530624	0.159699341
450.15	0.12928982	0.133013895	0.136738	0.140462044	0.14418612	0.147910193	0.1516343	0.155358	0.159082417	0.162806491

The thermal conductivity of soybean oil given in Table VII – VIII for biodiesel used in this work was gotten from the work of (Rojas et al., 2013), in which the critical properties of No. 2 diesel were obtained from the GT-Power fuel library. GT-Power combustion simulations require fuel properties in both liquid and vapour states. The fuel properties calculated by interpolation are for "liquid" state only. The dynamic and thermal conductivity array of Diesel No. 2 for vapour state in the GT library were assumed for biodiesel.

A. Fluid Dynamics Governing Equations

The need for a high accuracy result, high rate of calculation and generality are some of the criteria considered in selecting the engine models used in GT-Power software. The

parameters of fuel in the cylinder of an engine are defined by step by step solution of the system of differential equations of conservation of energy, mass and equation of state for open thermodynamic systems. Also, the dependence of the properties of gas on composition and temperature is taken into account. Some of the basic equations used in the software are defined by equation (1) to (19) from [19].

The conservation equations solved by GT-POWER are shown below:

Mass conservation is defined as the rate of change in mass within a subsystem which is equal to the sum of $\dot{m}$ from the system $\frac{d\dot{m}}{dt}$:

$$Continuity: \frac{dm}{dt} = \sum_{boundaries} \dot{m} \quad (1)$$

Energy conservation is defined as the rate of change of energy in a subsystem is equal to the sum of the energy transfer of the system:

$$Energy: \frac{d(me)}{dt} = P_{dt}^{dV} + \sum_{boundaries} (\dot{m}H) - hA_s(T_{fluid} - T_{wall}) \quad (explicit\ solver) \quad (2)$$

$$Enthalpy: \frac{d(\rho HV)}{dt} = V_{dt}^{dP} + \sum_{boundaries} (\dot{m}H) - hA_s(T_{fluid} - T_{wall}) \quad (implicit\ solver) \quad (3)$$

Momentum conservation, the net pressure forces and wall shear forces acting on a subsystem are equal to the rate of change of momentum in the system:

$$Momentum: \frac{d\dot{m}}{dt} = \frac{dPA + \sum_{boundaries}(\dot{m}u) - 4C_f \frac{\rho u|u|}{2}\frac{dxA}{D} - C_p\left(\frac{1}{2}\rho u|u|\right)A}{dx} \quad (4)$$

Where: $\dot{m}$ is the boundary mass flux into volume, $\dot{m} = \rho Au$, m is the mass of the volume, V is the volume, P is the pressure, ρ is the density, A is the cross-sectional flow area, A_s is the heat transfer surface area, e is the total specific internal energy (internal energy plus kinetic energy per unit mass), H is the total specific enthalpy, $H = e + \frac{P}{\rho}$, h is the heat transfer coefficient, T_{fluid} is the fluid temperature, T_{wall} is the wall temperature, u is the velocity at the boundary, C_f is the fanning friction factor, C_p is the pressure loss coefficient (commonly due to bend, taper or restriction), D is the equivalent diameter, dx is the length of mass element in the flow direction (discretization length), dP is the pressure differential acting across, dx.

B. Heat Transfer

1) Heat and Surface Roughness Loss: The heat transfer from fluids inside of pipes and flow split to their walls is calculated using a heat transfer coefficient. The heat transfer coefficient is calculated at every timestep from the fluid velocity, the thermo-physical properties and the wall surface roughness. The heat transfer coefficient of smooth pipes is calculated using the Colburn analogy.

$$h_g = \left(\frac{1}{2}\right) C_f \rho U_{eff} C_P Pr^{(-2/3)} \quad (5)$$

Where: C_f = Fanning friction factor of smooth pipe, ρ = density, U_{eff} = effective velocity outside boundary layer, C_P = specific heat, Pr = Prandtl number. The heat transfer coefficient of rough pipes is calculated using eq. (6)

$$h_{g,rough} = h_g \left[\frac{C_{f,roug}}{C_f}\right]^n \quad (6)$$

$h_{g,rough}$ is heat transfer coefficient of rough pipe and $C_{f,rough}$ is the fanning friction factor of rough pipe.

2) In-Cylinder Heat Transfer Model: The WoshniGT model relationship was adopted. The swirl and tumble coefficients are considered zero when this model is used. The heat transfer is determined as eq. (7)

$$\dot{Q} = h_c A_{cw}(T_{cw} - T_c) \quad (7)$$

The convective heat transfer coefficient for the WoschniGT model is given below:

$$h_{c(WoschniGT)} = \frac{K_1 p^{0.8} w^{0.8}}{B^{0.2} T^{K_2}} \quad (8)$$

C. Valve Modelling

The valve angle and lift array data should be consistent with the angle and lift attributes so that valve position, ϕ, is specified relative to TDC firing as in the following equations:

$$standard: \phi_{TDCF} = \phi_{array} * AngleMultiplier + CamTimingAngle \quad (9)$$

$$opening: \phi_{TDCF} = (\phi_{array} - \phi_{fdp}) * AngleMultiplier + CamTimingAngle + \phi_{fdp} \quad (10)$$

$$closing: \phi_{TDCF} = (\phi_{array} - \phi_{idp}) * AngleMultiplier + CamTimingAngle + \phi_{idp} \quad (11)$$

$$opening: \phi_{TDCF} = (\phi_{array} - \phi_{ml}) * AngleMultiplier + CamTimingAngle + \phi_{ml} \quad (12)$$

Where ϕ_{array}represents the array of angles where the valve is open, ϕ_{fdp} is the first data point, ϕ_{idp} the last point and ϕ_{ml} is the maximum lift.

D. Combustion Modelling

'EngCylCombDIWiebe', normally non-predictive model, imposes the burn rate for direct-injection, compression-ignition engines using a three-term Wiebe function, the superposition of three normal Wiebe curves. These Wiebe curves approximate the "typical" shape of a DI compression ignition burn rate. The purpose of using three functions is to make it possible to model pre-ignition and larger tail. This model should be used only (Gamma Technology, 2006) when the fuel is injected directly into the cylinder with an 'InjProfileConn' connection.

The Wiebe equations are given below:

Inputs : *SOI* = Start of Injection, *ID* = Ignition Delay, D_P = Premix Duration, D_M = Main Duration D_T = Tail Duration, F_P =Premix Fraction, F_T = Tail Fraction, E_P = Premix Exponent, E_M =Main Exponent, E_T =Tail Exponent, *CE*= Fraction of fuel burned (also known as "Combustion Efficiency")

Calculated constants: F_M =Main Fraction, WC_P =Wiebe Premix Constant, WC_M = Wiebe Main Constant, WC_T =Wiebe Tail Constant

The relation between the fractions is given below:

$$F_M = (1 - F_P - F_T) \tag{13}$$

The calculated constants are presented in the following equations:

$$WC_P = \left[\frac{D_P}{2.302^{1/(E_P+1)} - 0.105^{1/(E_P+1)}}\right]^{-(E_P+1)} \tag{14}$$

$$WC_M = \left[\frac{D_M}{2.302^{1/(E_M+1)} - 0.105^{1/(E_M+1)}}\right]^{-(E_M+1)} \tag{15}$$

$$WC_T = \left[\frac{D_T}{2.302^{1/(E_T+1)} - 0.105^{1/(E_T+1)}}\right]^{-(E_T+1)} \tag{16}$$

Burn Rate Calculation

$$\theta = Instantaneous\ Crank\ Angle$$

The cumulative burn rate is calculated, normalized to 1.0. The combustion starts at 0.0 (0.0% burned) and progresses to the value specified by the "Fraction of Fuel Burned Attribute", which is typically 1.0 or 100%.

$$\begin{aligned} &Combustion(\theta) \\ &= (CE)(F_p)\left[1 - e^{-(WC_p)(\theta - SOI - ID)^{(E_p+1)}}\right] \\ &+ (CE)(F_M)\left[1 - e^{-(WC_M)(\theta - SOI - ID)^{(E_M+1)}}\right] \\ &+ (CE)(F_T)\left[1 - e^{-(WC_T)(\theta - SOI - ID)^{(E_T+1)}}\right] \end{aligned} \tag{17}$$

E. Emission Modelling

The modelling of NOx emissions is achieved by using the Extended Zeldovich mechanism as utilized by [21] :

$$\begin{aligned} &N + NO \leftrightarrow N_2 + O \\ &N + O_2 \leftrightarrow NO + O \\ &N + OH \leftrightarrow NO + H \end{aligned} \tag{18}$$

F. Friction Modelling

Chen and Flynn recognized that the frictional losses will not only be dependent on mean piston speed but also on the peak cylinder pressure, through its influence on bearing loads [22]. Friction Mean Effective Pressure is given by the following equation:

$$\begin{aligned} FMEP = C + (PF * P_{max}) + \left(MPSF * Speed_{mp}\right) \\ + \left(MPSSF * Speed_{mp}^2\right) \end{aligned} \tag{19}$$

Where: FMEP = Friction Mean Effective Pressure, P_{max} = Maximum cylinder pressure, $Speed_{mp}$ = mean piston speed, C = Constant part of FMEP, PF = Peak cylinder pressure factor, $MPSF$ = Mean piston speed factor, $MPSSF$ = Mean piston speed squared factor. The FMEP is estimated by means of an empirically derived model that approximates the total engine friction as function of peak cylinder pressure, mean piston speed and mean piston speed squared.

III. RESULTS AND DISCUSSION

GT-Power software has been used for investigating the impact of injection timing and various blending ratios on performance and emissions characteristics of a compression ignition engine at full load conditions by varying engine speed. Four injection timings namely retarded 21 CA bTDC, original 23 CA bTDC, and advanced 25 and 27 CA bTDC were tried. Blend B5, B10, B15, B20, B25, B30, B35, B40, B45, B50, B55, B60, B65, B70, B75, B80, B85, B90, B95 as well as pure biodiesel (B100) and diesel has been used in this work. The result generated is presented in the form of a graph with the brake mean effective pressure, brake specific fuel consumption, brake efficiency, brake torque, brake power, NOx, CO, CO_2, and HC plotted against varying engine speed between the range of 1000 – 5000 rpm.

A. Performance Characteristics

The result of the effect of blend ratio and injection timing on performance parameters such as brake mean effective pressure, brake specific fuel consumption, brake efficiency, brake torque and brake power are discussed in this section.

1) Brake Mean Effective Pressure: The brake mean effective pressure (BMEP) is the external shaft work per unit volume done by the engine. The variation of BMEP with an engine speed for different Tropical almond seed biodiesel blends at various injection timings are shown in fig. 2 - 5. The BMEP increases with increase in speed up to 4000 rpm, afterwards, decreases over the entire range of engine speed. The BMEP for all blends is higher than the diesel for all engine speeds and injection timings. The highest BMEP is obtained at 4000rpm with B35 due to fuel properties such as

heat of vaporization (Bhuiya et al., 2019) because the molecules of a liquid are in constant motion and possess a wide range of kinetic energies, at any moment some fraction of them has enough energy to escape from the surface of the liquid to enter the gas or vapour phase. At original injection timing, the BMEP for B35 is higher by about 9.16% than that of diesel at the slower speed due to the properties of the fuel. BMEP is higher by about 5.67%, at retarding injection timing of 21CA bTDC; 6.36% and 6.74% at advancing injection timing of 25 and 27 CA bTDC respectively, compared to that of the original injection timing of 6.01% at maximum speed.

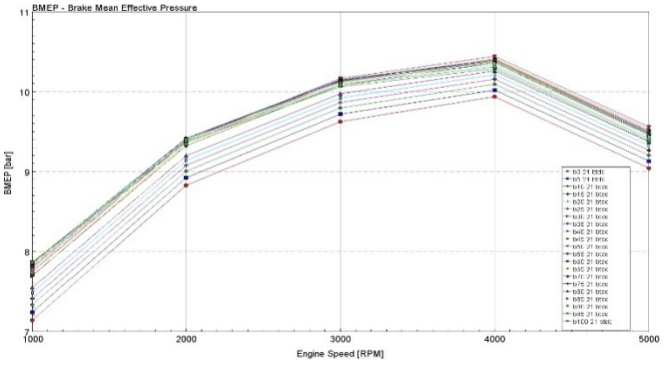

Fig. 2 Brake mean effective pressure vs. Engine speed for injection timing 21CA

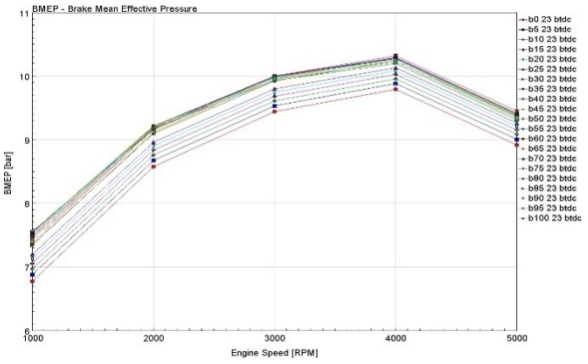

Fig. 3 Brake mean effective pressure vs. Engine speed for injection timing 23CA

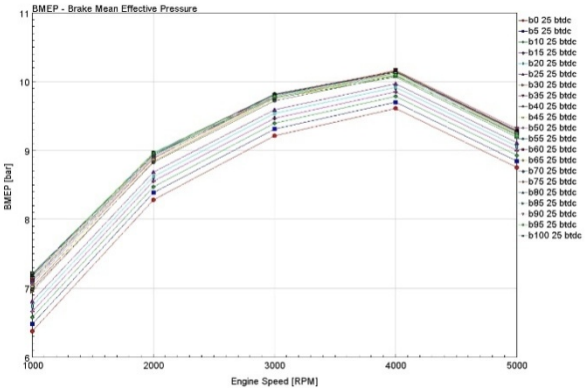

Fig. 4 Brake mean effective pressure vs. Engine speed for injection timing 25CA

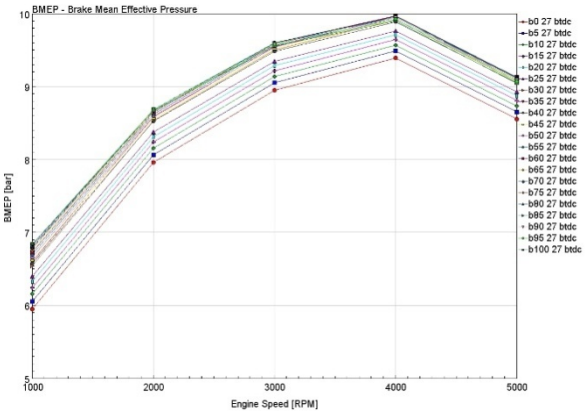

Fig. 5 Brake mean effective pressure vs. Engine speed for injection timing 27CA

2) *Brake Specific Fuel Consumption:* BSFC is a measure of the fuel efficiency of any engine that burns fuel and produces rotational power output. The BSFC value indicates how efficiently the engine converts fuel supplied into useful work. The variation of BSFC with an engine speed for different Tropical almond seed biodiesel blends at various injection timings are shown in fig. 6 – 9. At original injection timing, the BSFC for B35 is lower by about 8.39% than that of diesel at the lower speed due to calorific value and oxygen content present in the fuel because the higher the calorific value, the lower the BSFC and a higher oxygen content of biodiesel helps to facilitate better combustion [24]. BSFC is lower by about 5.67%, 5.98%, and 6.32% at retarded and advanced timing of 21; 25 and 27 CA bTDC respectively, compared to that of the original injection timing of 5.37% at maximum speed. The specific fuel consumption and engine efficiency are inversely related, so that the lower the specific fuel consumption, the higher the engine efficiency. In general, the BSFC is found to decrease with raising the biodiesel quantity in the blends with B35 being the lowest at the maximum speed of 4000 rpm (21-25 CA bTDC) and 5000 rpm (27CA bTDC).

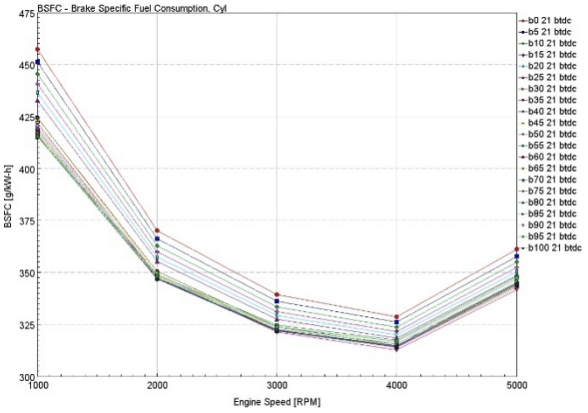

Fig. 6 BSFC vs. Engine speed for injection timing 21CA

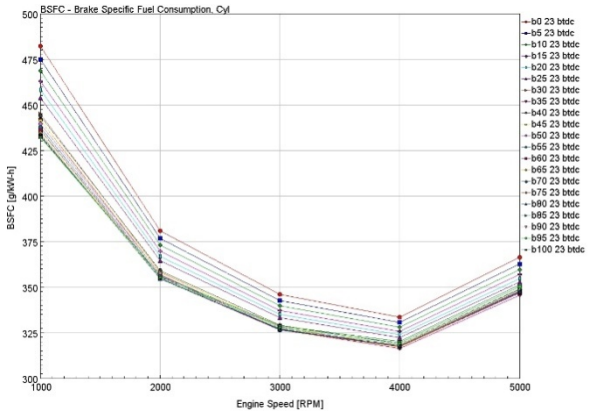

Fig. 7 BSFC vs. Engine speed for injection timing 23CA

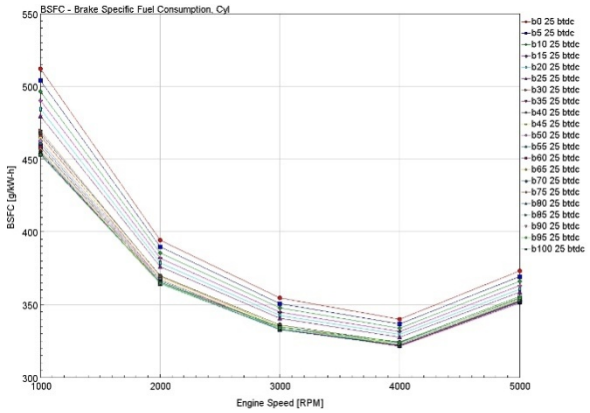

Fig. 8 BSFC vs. Engine speed for injection timing 25CA

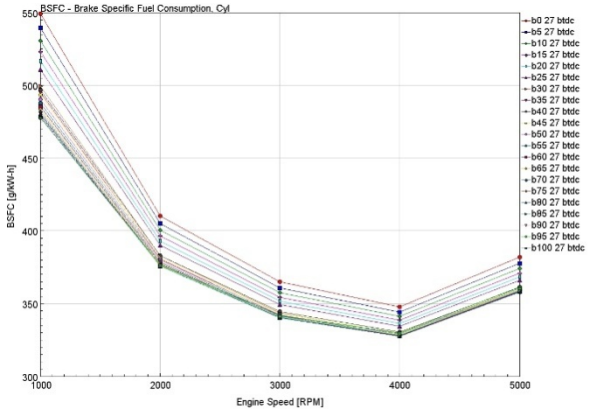

Fig. 9 BSFC vs. Engine speed for injection timing 27CA

3) *Brake Efficiency:* The variation of brake efficiency with an engine speed for different tropical almond seed biodiesel blends at various injection timings is shown in fig. 10 – 13. It can be observed that tropical almond seed oil biodiesel and its blend behaves similarly with diesel. The brake efficiency increases with increase in speed up to 4000 rpm, afterwards, decreases over the entire range of engine speed. The brake efficiency for all blends is higher than the diesel for all engine speeds and injection timings. Also, an increasing trend of brake efficiency with increasing blend ratio was noticed for tropical almond seed oil-based biodiesel at low and high engine speeds with B100 being the highest. The highest brake efficiency is obtained at 4000rpm with B35 due to fuel properties. As seen in figure 4.5 at the 23CA original injection timing, the brake efficiency of A35 is higher by about 14.23% than that of diesel at low speed. It can also be observed that the advanced injection timings at 25CA and 27CA give a higher brake efficiency of 11.30% and 11.70% than those of the original and retarded injection timings of 10.94% and 10.58% respectively at full speed.

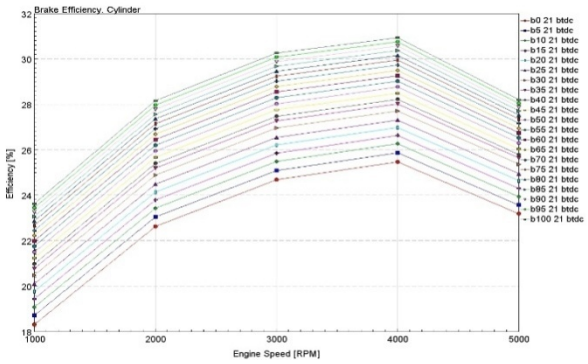

Fig. 10 BE vs. Engine speed for injection timing 21CA

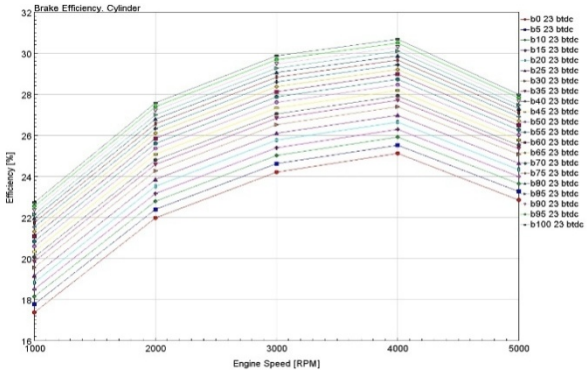

Fig. 11 BE vs. Engine speed for injection timing 23CA

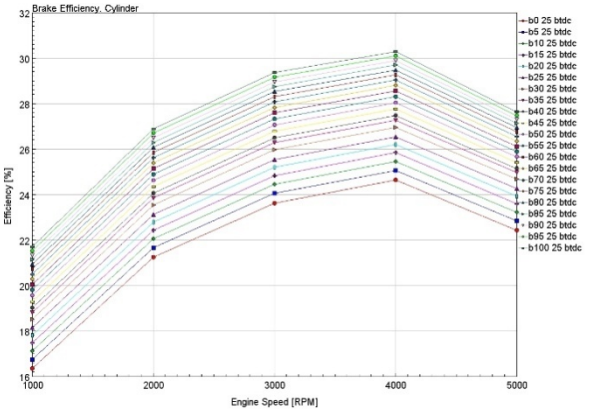

Fig. 12 BE vs. Engine speed for injection timing 25CA

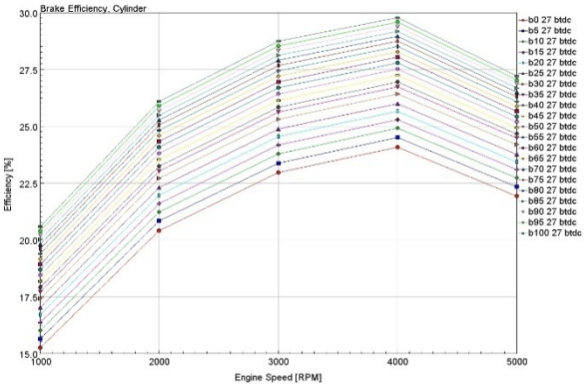

Fig. 13 BE vs. Engine speed for injection timing 27CA

4) *Brake Torque:* Torque is a measure of the capacity to produce a running engine and is used to overcome obstacles along the way or to increase engine speed. The variation of brake torque with an engine speed for different tropical almond biodiesel blends at various injection timings is shown in fig. 14 – 17. It can be observed that tropical almond seed oil biodiesel and its blend behaves similarly with diesel. The brake torque increases with increase in speed up to 4000 rpm, afterwards, decreases over the entire range of engine speed, caused by turbulent flow into the combustion chamber which is higher as the increase in engine speed to enhance fire propagation. While the tendency to decrease the torque on the engine speed above 4000 rpm due to increased friction losses, heat losses and incomplete combustion process. The brake torque for all blends is higher than the diesel for all engine speeds and injection timings [25]. The highest brake torque is obtained at 4000rpm with B35. This can be due to B35 contribution to atomization and heat release. At original injection timing, the BT for B35 is higher by about 9.16% than that of diesel at the lower speed due to the properties of the fuel. BP is higher by about 5.67%, at retarding injection timing of 21CA bTDC; 6.36% and 6.74% at advancing injection timing of 25 and 27 CA bTDC respectively, compared to that of the original injection timing of 6.01% at maximum speed.

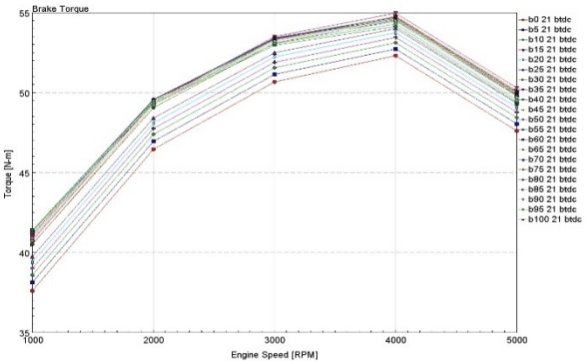

Fig. 14 BT vs. Engine speed for injection timing 21CA

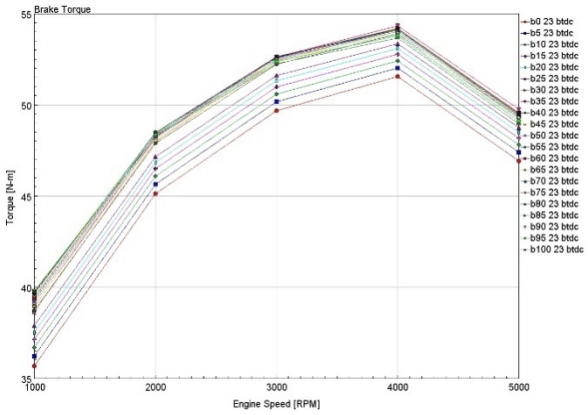

Fig. 15 BT vs. Engine speed for injection timing 23CA

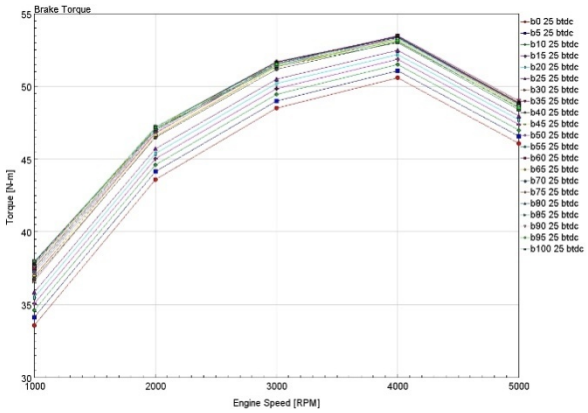

Fig. 16 BT vs. Engine speed for injection timing 25CA

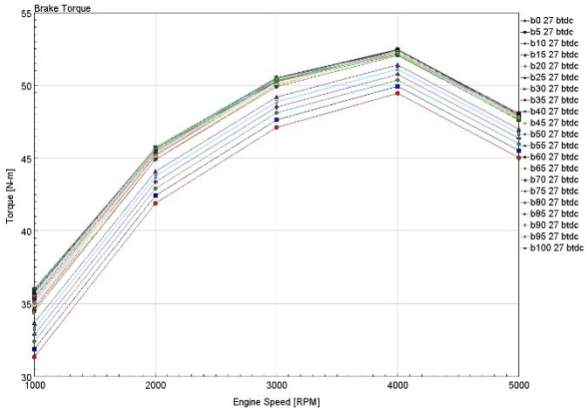

Fig. 17 BT vs. Engine speed for injection timing 27CA

5) *Brake Power:* The variation of brake power with an engine speed for different Tropical almond seed biodiesel blends at various injection timings are shown in fig. 18 – 21. It can be observed that tropical almond seed oil biodiesel and its blend behaves similarly with diesel. The brake power increases with increasing engine speed with the maximum brake power at the maximum investigated engine speed. Also, an increasing trend of brake power with increasing blend ratio was noticed for tropical

almond seed oil-based biodiesel at low and high engine speeds. At original injection timing (23 CA) the brake power for B35 is higher by about 9.16% than that of diesel at the lower speed due to higher cetane number of B35 leading to shorter ignition delays and requiring less time for the fuel combustion process to be completed [26]. Brake power is higher by about 6.74% and 6.36% at advancing injection timing of 27CA bTDC and 25CA bTDC respectively, while it is higher by about 5.67% with the retarded injection timing of 21CA bTDC, compared to that of the original injection timing of 6.01% at maximum speed. As a result, maximum brake power was obtained at advanced injection timings for B35. While retarding the injection timing combustion is incomplete that results in a lower brake power at maximum speed, than that of the original injection timing. In general, the brake power is found to increase with raising the biodiesel quantity in the blends with B35 being the highest at the maximum speed of 5000 rpm at all injection timings.

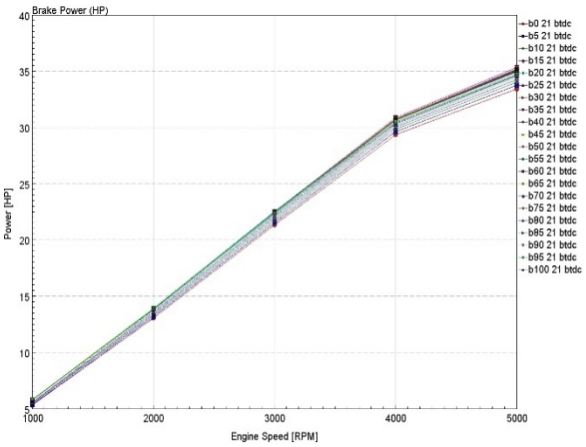

Fig. 18 BP vs. Engine speed for injection timing 21CA

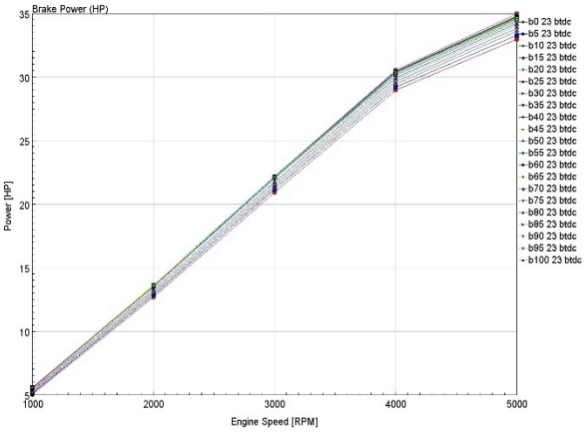

Fig. 19 BP vs. Engine speed for injection timing 23CA

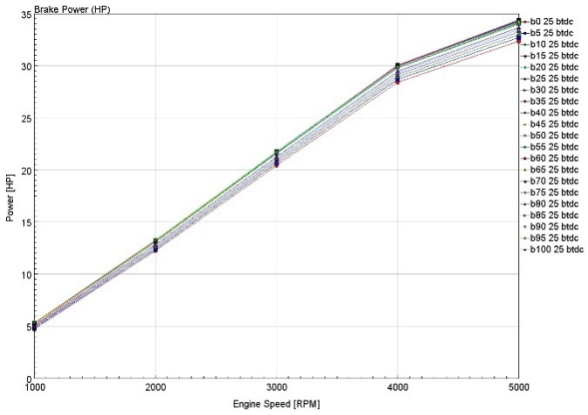

Fig. 20 BP vs. Engine speed for injection timing 25CA

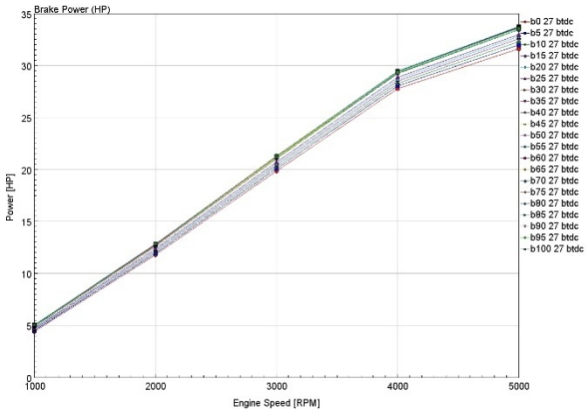

Fig. 21 BP vs. Engine speed for injection timing 27CA

B. Emission Characteristics

Emission parameters investigated in this work include Oxides of nitrogen, Carbon monoxide, Carbon dioxide, and Hydrocarbon. The NOx, CO, CO_2, and HC are plotted against the engine speed.

1) Carbon Monoxide: CO discharges are formed because of the incomplete combustion of petroleum fuels that contain no oxygen in their molecular structure. Also, the low in-cylinder temperature causes a cooling impact that too favours the formation of CO emissions. The variation of carbon monoxide emission with an engine speed for different tropical almond biodiesel blends at various injection timings is shown in fig. 22 – 25. It can be observed that tropical almond seed oil biodiesel and its blend behaves similarly with diesel. The CO decreases with increasing engine speed with the minimum CO at 4000 rpm investigated engine speed. Also, a decreasing trend of CO with increasing blend ratio was noticed for tropical almond seed oil-based biodiesel at low and high engine speeds with B100 being the lowest. As seen in Figure 4.8 at the 23CA original injection timing, the CO emission of A35 is lower by about 30.36% than that of diesel at low speed. This decrease could be attributed to

the biodiesels having higher oxygen content than diesel which can result in more complete combustion, leading to less CO in the exhaust stream [27]. It can also be observed that the advanced injection timings at 25CA and 27CA give a lower CO emission of 31.22% and 31.41% than those of the original and retarded injection timings of 30.99% and 30.78% respectively at full speed.

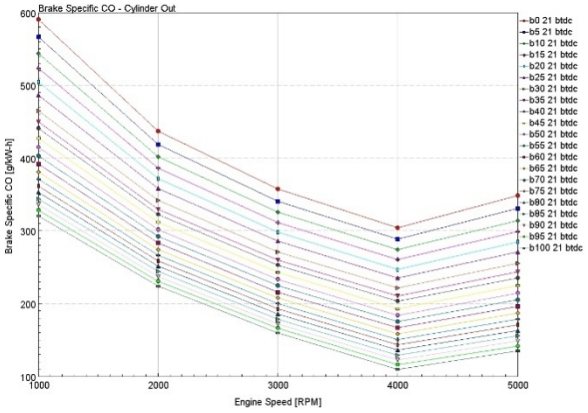

Fig. 22 CO vs. Engine speed for injection timing 21CA

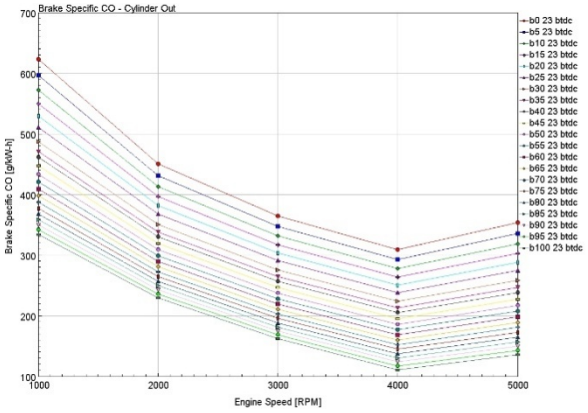

Fig. 23 CO vs. Engine speed for injection timing 23CA

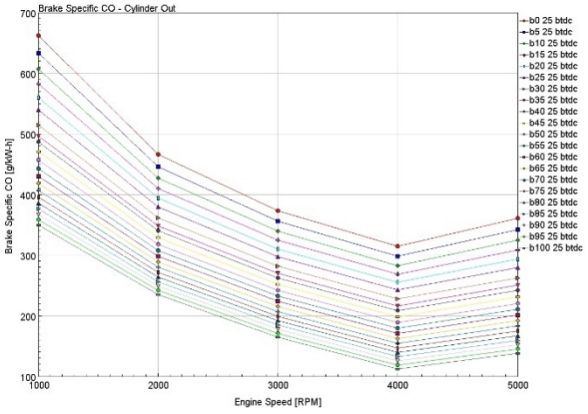

Fig. 24 CO vs. Engine speed for injection timing 25CA

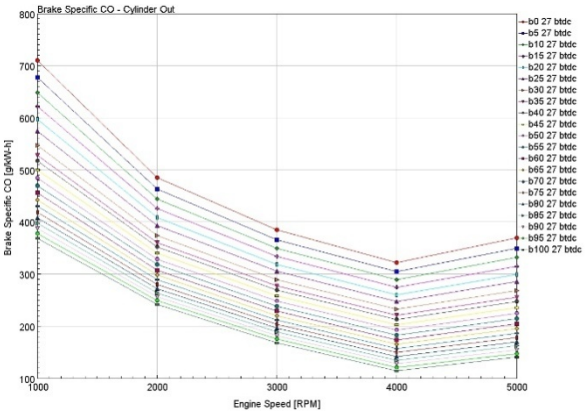

Fig. 25 CO vs. Engine speed for injection timing 27CA

2) *Hydrocarbon:* Hydrocarbon emissions result from the release of unburned or partially combusted hydrocarbon fuels. The variation of hydrocarbon emission with an engine speed for different tropical almond biodiesel blends at various injection timings is shown in fig. 26 – 29. It can be observed that tropical almond seed oil biodiesel and its blend behaves similarly with diesel. HC emission decreases with an increase in engine speed for diesel and B35 with 4000 rpm being the lowest and a spike at 5000 rpm for all injection timings due to complete combustion. HC emission at 1000 rpm is higher due to decreased fuel vaporization and oxidation of the fuel [28]. B35 gives a lower HC emission for advanced injection timings at all speeds. It is believed that the longer ignition delay enhances the formation of local rich-fuel zones on the cylinder walls, which are not able to burn completely [29]. Also, B35 gives a lower HC emission for advanced injection timings at maximum investigated speed about diesel. Advancing the injection timing causes an earlier start of combustion relative to the TDC. Because of this, the cylinder charge is being compressed as the piston moves to the TDC, and that results in relatively higher temperatures, and thus reduces the HC emissions.

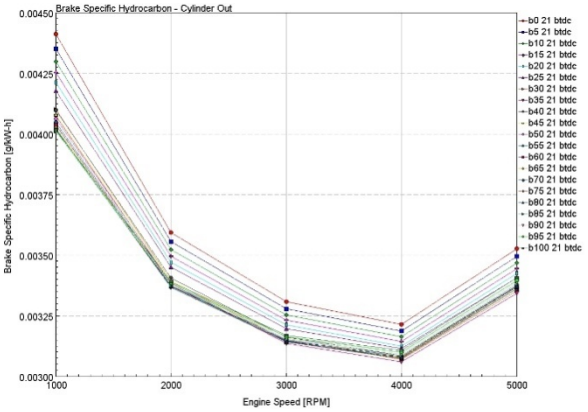

Fig. 26 HC vs. Engine speed for injection timing 21CA

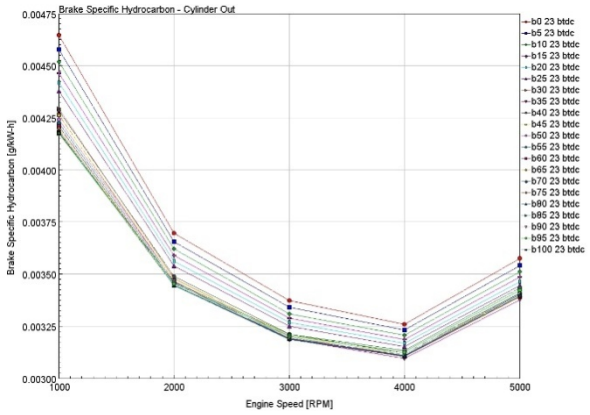

Fig. 27 HC vs. Engine speed for injection timing 23CA

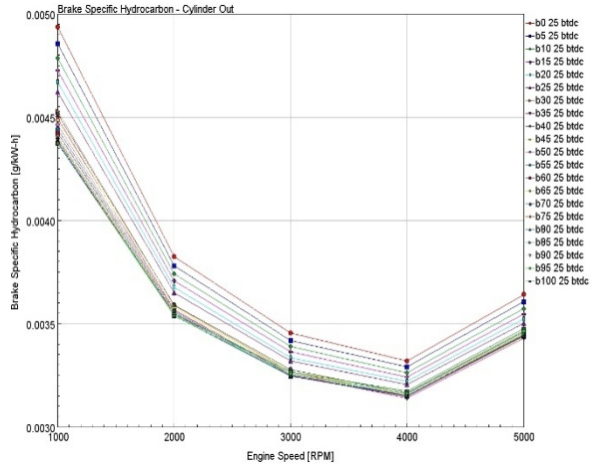

Fig. 28 HC vs. Engine speed for injection timing 25CA

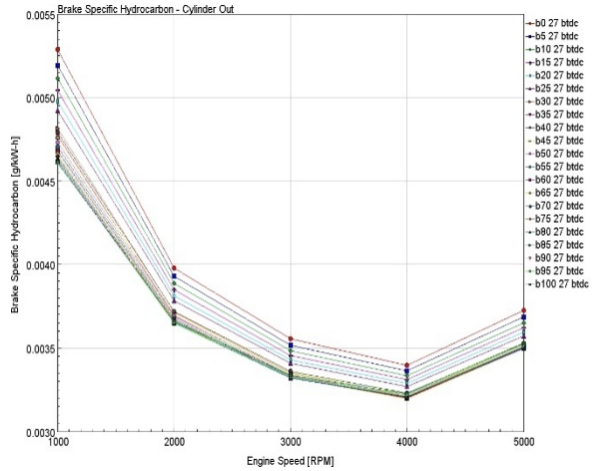

Fig. 29 HC vs. Engine speed for injection timing 27CA

3) Carbon Dioxide: Carbon dioxide (CO_2), a primary gaseous combustion product of internal combustion engines, is also a greenhouse gas and is in the process of being regulated as well, due to its increasing atmospheric concentration [28]. The variation of carbon dioxide emission with an engine speed for different tropical almond biodiesel blends at various injection timings is shown in fig. 30 – 33. It can be seen that biodiesels display an increase in CO_2 emissions with increasing blend ratios with B100 being the highest at all injection timings. Also, lowest CO_2 emissions are observed at an engine speed of 2000 rpm for all tested fuels at all investigated injection timings. As seen in figure 4.10 at the 23CA original injection timing, the CO_2 emission of B35 is higher by about 7.29% than that of diesel at full speed. This increase could be attributed to the biodiesels having higher oxygen content than diesel. It can also be observed that the advanced injection timings at 25CA and 27CA give a higher CO_2 emission than those of the original and retarded injection timings at full speed. More fuel injection at higher speeds, increased combustion temperature and oxidation rates are responsible for the higher CO_2 at advanced injection timing. The results conform to those in the literature (Peterson et al., 1996; Sheehan et al., 1998).

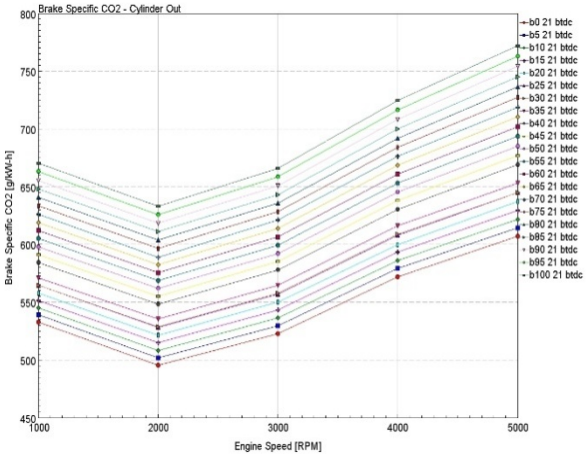

Fig. 30 CO_2 vs. Engine speed for injection timing 21CA

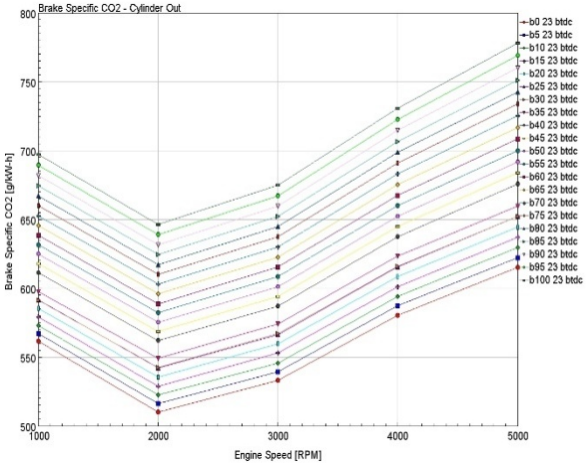

Fig. 31 CO_2 vs. Engine speed for injection timing 23CA

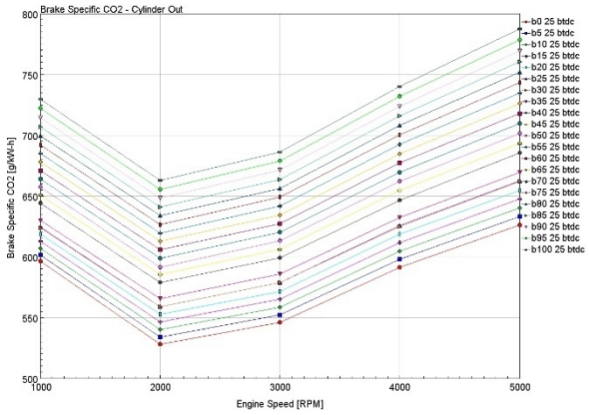

Fig. 32 CO_2 vs. Engine speed for injection timing 25CA

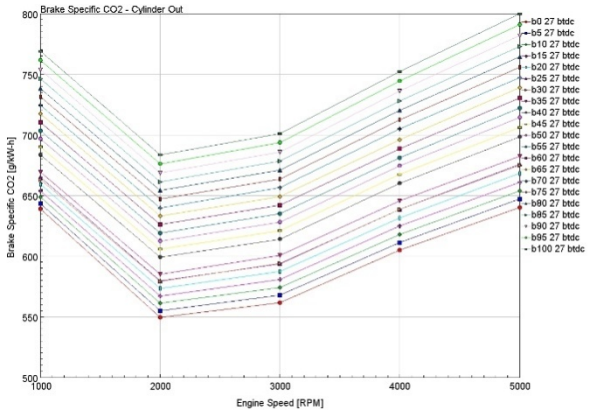

Fig. 33 CO_2 vs. Engine speed for injection timing 27CA

4) *Oxides of Nitrogen:* Nitrogen oxides (NOx) are formed throughout the combustion chamber during the combustion process due to the disassociation of N_2 and O_2 into their atomic states and subsequent reactions with molecular oxygen and nitrogen. The variation of oxides of nitrogen with an engine speed for different tropical almond biodiesel blends at various injection timings is shown in fig. 34 – 37. It can be seen that biodiesels display an increase in NOx emissions with B100 being the highest from 2000 to 5000 rpm at all injection timings. This can vary due to higher oxygen content in biodiesel and higher temperature in the engine cylinder. Also, the lowest NOx emission is observed at an engine speed of 1000 rpm for all tested fuels with diesel being the highest at all investigated injection timings. As the reactions forming NOx are highly temperature-dependent, so NOx emissions are relatively low during engine start and warm-up, and then scale proportionally with the engine speed [28]. As seen in figure 4.11 at the 23CA original injection timing, the NOx emission of B35 is lower by about 6.80% than that of diesel at low speed. It can also be observed that the advanced injection timings at 25CA and 27CA give a higher NOx emission of 0.90% and 0.44% than those of the original and retarded injection timings of 1.34% and 1.79% respectively at full speed.

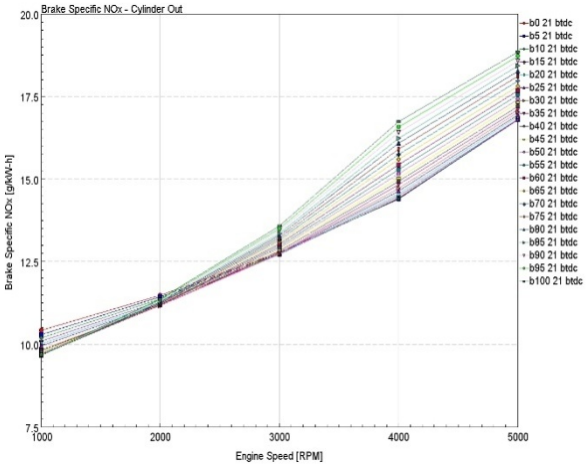

Fig. 34 NO_X vs. Engine speed for injection timing 21CA

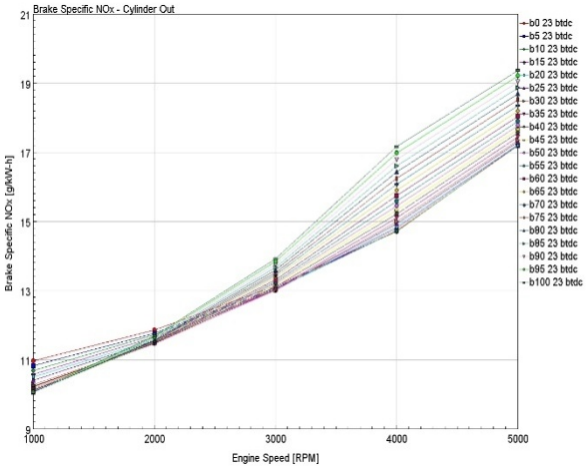

Fig. 35 NO_X vs. Engine speed for injection timing 23CA

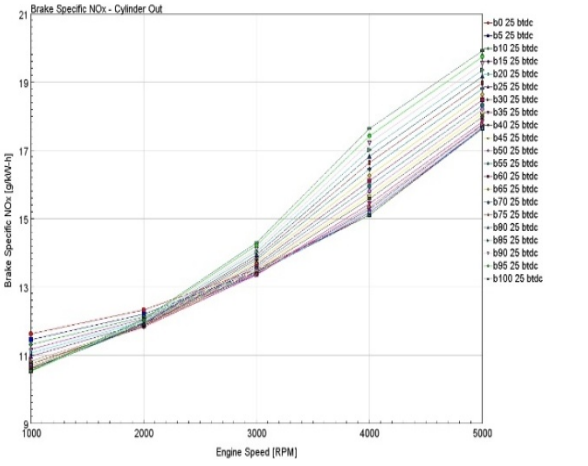

Fig. 36 NO_X vs. Engine speed for injection timing 25CA

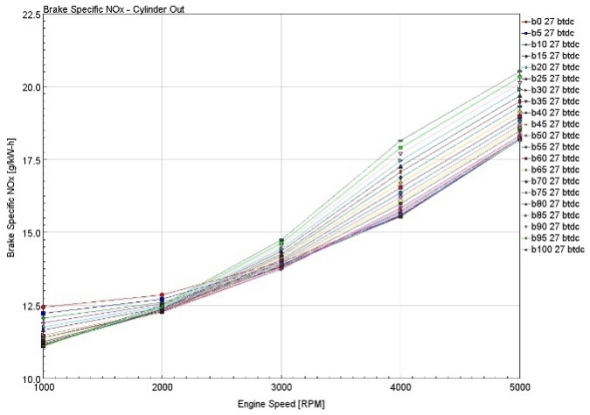

Fig. 37 NO_X vs. Engine speed for injection timing 27CA

IV. CONCLUSIONS

This study has been able to ascertain the influence of varying injection timing on performance and emission characteristics of a compression ignition engine fuelled with tropical almond seed oil-based biodiesel and its blends; the following conclusions have been established:

i) For all blends tested, B35 provides the best result in terms of HC, BP, BT, ISFC, BSFC, IMEP and BMEP for all investigated injection timings. Therefore, B35 can be used as alternative biodiesel.

ii) Highest brake power exists at the highest engine speed in the investigation.

iii) It was observed that the best injection timing was 27CA bTDC. Hence B35 can be effectively used as alternative biodiesel with an injection timing of 27CA bTDC in compression ignition engines. It was also observed that there was an increase in BE, BMEP, IMEP, BT, BP, CO_2 and a decrease in BSFC, ISFC, HC and CO.

iv) Also, NOx emissions are increased significantly with increased biodiesel content. This phenomenon occurs due to the higher stoichiometry of biodiesel fuel blends than those of traditional diesel, causing the enhanced formation of NOx emissions.

In general, advancing injection timing had more benefit to tropical almond seed oil-based biodiesel and its blends in terms of their performance and emission characteristics.

REFERENCES

[1] B. A. Orhevba, S. E. Adebayo, and A. O. Salihu, "Synthesis of Biodiesel from Tropical Almond (Terminalia Catappa) Seed Oil," *Curr. Res. Agric. Sci.*, vol. 3, no. 4, pp. 57–63, 2016.

[2] P. Lingfa, "A Comparative Study on Performance and Emission Characteristics of Compression Ignition Engine using Biodiesel Derived from Castor oil Abstract :," *Int. J. Innov. Res. Sci. Eng. Technol.*, vol. 3, no. 4, pp. 124–128, 2014.

[3] K. S. Babulal, A. Pradeep, and P. Muthukumar, "Experimental Performance and Emission Analysis of C . I Engine Fuelled with Biodiesel," *Int. J. Innov. Res. Sci. Eng. Technol.*, vol. 4, no. 2, pp. 133–138, 2015.

[4] R. Narsinga and K. Ranjith, "Effect of Fuel Injection Pressure and Injection Timing on Performance and Emissions of Diesel Engine Using Nanoadditive Blends," *J. Appl. Sci. Innov.*, vol. 1, no. 4, pp. 5–13, 2017.

[5] J. Hwang, D. Qi, Y. Jung, and C. Bae, "Effect of injection parameters on the combustion and emission characteristics in a common-rail direct injection diesel engine fueled with waste cooking oil biodiesel," *Renew. Energy*, vol. 63, pp. 9–17, 2014.

[6] G. R. Kannan and R. Anand, "Effect of injection pressure and injection timing on DI diesel engine fuelled with biodiesel from waste cooking oil," *Biomass and Bioenergy*, vol. 46, pp. 343–352, 2012.

[7] R. L. Krupakaran, T. Hariprasasd, and A. Gopalakrishna, "Influence of injection timing on engine performance, emission characteristics of Mimusops Elangi methyl ester," *Int. J. Ambient Energy*, vol. 0750, no. May, pp. 1–10, 2018.

[8] G. J. Rani, Y. V. H. Rao, and B. Balakrishna, "Fuel Injection Timing impact on diesel engine performance , combustion and emission characteristics of nano additive biodiesel blends," *Int. J. Ambient Energy*, vol. 0, no. 0, pp. 1–21, 2020.

[9] N. Karthik, R. Rajasekar, R. Siva, and G. Mathiselvan, "Experimental investigation of injection timing on the performance and exhaust emissions of a rubber seed oil blend fuel in constant speed diesel engine," *Int. J. Ambient Energy*, vol. 40, no. 3, pp. 292–294, 2019.

[10] J. Jayaprabakar, A. Karthikeyan, and V. Rameshkumar, "Effect of injection timing on the combustion characteristics of rice bran and algae biodiesel blends in a compression-ignition engine," *Int. J. Ambient Energy*, vol. 38, no. 2, pp. 116–121, 2017.

[11] M. Harun Kumar, V. Dhana Raju, P. S. Kishore, and H. Venu, "Influence of injection timing on the performance, combustion and emission characteristics of diesel engine powered with tamarind seed biodiesel blend," *Int. J. Ambient Energy*, vol. 0, no. 0, pp. 1–31, 2018.

[12] P. Karthikeyan, P. Lokesh, and P. Suneel, "Performance and emission characteristics of direct injection diesel engine using linseed oil as biodiesel by varying injection timing," *Int. J. Ambient Energy*, vol. 40, no. 1, pp. 35–39, 2019.

[13] S. K. Fasogbon, O. O. Laosebikan, and C. U. Owora, "ANN Analysis of Injection Timing on Performance Characteristics of Compression Ignition Engines Running on the Blends of Tropical Almond Based Biodiesel," *Am. J. Mod. Energy*, vol. 5, no. 2, pp. 40–48, 2019.

[14] R. Rahim, R. Mamat, and M. Y. Taib, "Comparative Study on Diesel Engine Performance Operating With Biodiesel and Diesel Fuel," *Natl. Conf. Mech. Eng. Res. Postgrad. Stud. (2nd NCMER 2010)*, no. December, pp. 863–870, 2010.

[15] S. K. Fasogbon and M. F. Odia, "Modelling Combustion Characteristics of a Turbocharged Low Heat Rejection Direct Injection Compression Ignition Engine Fuelled with methyl Ester of Seed Oil of Terminalia Catappa L . and its Blends," *Int. J. Latest Technol. Eng. Manag. Appl. Sci.*, vol. VIII, no. Iii, pp. 49–54, 2019.

[16] S. N. Sahasrabudhe, V. Rodriguez-Martinez, M. O'Meara, and B. E. Farkas, "Density, viscosity, and surface tension of five vegetable oils at elevated temperatures: Measurement and modeling," *Int. J. Food Prop.*, vol. 20, no. 2, pp. 1965–1981, 2017.

[17] O. O. Fasina and Z. Colley, "Viscosity and specific heat of vegetable oils as a function of temperature: 35°C to 180°C," *Int. J. Food Prop.*, vol. 11, no. 4, pp. 738–746, 2008.

[18] E. E. G. Rojas, J. S. R. Coimbra, and J. Telis-Romero, "Thermophysical properties of cotton, canola, sunflower and soybean oils as a function of temperature," *Int. J. Food Prop.*, vol. 16, no. 7, pp. 1620–1629, 2013.

[19] E. Performance and A. Manual, "GT-SUITE," 2016.

[20] Gamma Technology, "Highlights : GT-POWER Engine Simulation Software Features and Applications."

[21] T. Morel and S. Wahiduzzaman, "morel denge.pdf," *Modeling of*

diesel combustion and emissions. FISITA Congress, June 1996., 1996.

[22] S. K. Chen and P. F. Flynn, "Development of a single cylinder compression ignition research engine," *SAE Tech. Pap.*, 1965.

[23] M. Bhuiya, M. Rasul, M. Khan, and N. Ashwath, "Performance and emission characteristics of a compression ignition Performance and emission characteristics of a compression ignition (CI) engine operated with beauty leaf biodiesel The 15th International Symposium on District Heating and Cooling Assessin," *Energy Procedia*, vol. 160, no. 2018, pp. 641–647, 2019.

[24] B. Ashok and K. Nanthagopal, *Eco friendly biofuels for CI engine applications*. Elsevier Ltd., 2019.

[25] B. Sudarmanta, "Influence of the compression ratio and ignition timing on Sinjai engine performance with 50 % bioethanol-gasoline blended fuel INFLUENCE OF THE COMPRESSION RATIO AND IGNITION TIMING ON SINJAI ENGINE PERFORMANCE WITH 50 % BIOETHANOL-," *ARPN J. Eng. Appl. Sci.*, vol. 11, no. February, 2016.

[26] M. I. Arbab, H. H. Masjuki, M. Varman, M. A. Kalam, S. Imtenan, and H. Sajjad, "Experimental Investigation of Optimum Blend Ratio of Jatropha , Palm and Coconut Based Biodiesel to Improve Fuel Properties , Engine Performance and Emission Characteristics," in *SAE Technical Paper Series*, 2013, no. October.

[27] P. Mccarthy, M. G. Rasul, and S. Moazzem, "Comparison of the performance and emissions of different biodiesel blends against petroleum diesel," *Int. J. Low-Carbon Technol.*, vol. 6, no. 4, pp. 255–260, 2011.

[28] C. R. Ferguson and A. T. Kirkpatrick, *Internal Combustion Engines Applied Thermosciences*, Third. John The Atrium, Southern Gate, Chichester, West Sussex, PO19 8SQ, United Kingdom: John Wiley & Sons, Ltd, 2016.

[29] I. Kalargaris, G. Tian, and S. Gu, "Influence of Advanced Injection Timing and Fuel Additive on Combustion , Performance , and Emission Characteristics of a DI Diesel Engine Running on Plastic Pyrolysis Oil," *J. Combust.*, vol. 2017, p. 9, 2017.

[30] C. L. PETERSON, D. L. REECE, J. C. THOMPSON, S. M. BECK, and C. CHASES, "ETHYL ESTER OF RAPESEED USED AS A BIODIESEL FUEL-A CASE STUDY *," *Biomass and Bioenergy*, vol. 10, no. 5–6, pp. 331–336, 1996.

[31] J. Sheehan, V. Camobreco, J. Duffield, M. Graboski, and H. Shapouri, "Life Cycle Inventory of Biodiesel and Petroleum Diesel for Use in an Urban Bus," 1998.